Laser-Wakefield Electron Accelerators

Adam A. S. Green

Department of Physics, University of Colorado at Boulder

May 12, 2015

Abstract

In the late 1970's, Tajima and Dawson published a seminal paper in *Physical Review Letters* outlining a new kind of electron accelerator that was orders of magnitude smaller than conventional technology. It worked by leveraging the high-energy gradients of laser-excited plasmas to accelerate electrons over centimeter length scales to GeV energies. Their proposal was untenable at the time as it required lasers with peak intensities far beyond the technology of the era. It has only been recently, through a combination of modern laser technology and powerful new numerical methods, that researchers have been able to make dramatic progress in the field. Several groups are now poised to deliver on the original promise of Tajima and Dawson.

In this work, we review the field of Laser Wakefield Plasma Accelerators (LWPA) covering the historical beginnings, the physical underpinnings, and close with a discussion of current

state-of-the-art experimental results.

Contents

1 Introduction

Conventional methods of electron acceleration use a TM-mode rf field propagating in a waveguide to provide the acceleration gradient. Waveg-

uide field gradients are fundamentally limited by electric breakdown on the walls of the waveguide to approximately a $\mathrm{MeV\,m^{-1}}$[1]. This means that to achieve the 50 GeV energies currently used at the Stanford Linear Accelerator Center (SLAC)[2], the waveguide has to be about 2 miles long. In contrast, the acceleration gradients in plasmas can easily exceed $10\,\mathrm{GeV\,m^{-1}}$, thereby allowing electrons to be accelerated over centimeters for similar energy gains[3]. The study of LWPA is strongly motivated by this promise of table-top electron accelerators.

The broadest application of high-energy electrons today is their use in free-electron x-ray lasers. The development of which has allowed investigation of structures in biology, solid state physics, as well as pioneering techniques in medical imaging[4, 5]. Currently, free-electron x-ray lasers are tied to the large linear accelerators that provide them with electrons. LWPA offers a smaller low-cost platform for electron acceleration, which would allow a broader use of x-ray lasers in the scientific community. The dissemination of more economical x-ray lasers would not only encourage more research but would also reduce the risk of limiting research due to damage or funding cuts to the larger, high-cost facilities[1]. Much like the impact of personal computers introduced in the era of massive supercomputers, the impact of a small cheap x-ray laser will be dramatic[6].

[1] The famous cancellation of the Superconducting Super Collider in Texas due to budget problems in one dramatic example.

The goal of LWPA technology is to produce a large number of high-energy electrons with a narrow energy distribution in a collimated

beam. It is an exciting time for LWPA as it is only within the past decade that LWPA technology became capable of meeting the above requirements.

1.1 History

Tajima and Dawson originally proposed shooting a high-intensity laser pulse at a plasma[7]. The photon-pressure of the laser generated a wakefield and electrons could 'surf' this wake and be accelerated. Unfortunately, the lasers of the day could not reach the high intensities required. It was the invention of chirped-pulse amplification (CPA) and resulting high-intensity lasers that allowed serious progress in the LWPA field to occur[8]. Even when the intensity issue had been overcome there were still severe experimental constraints, as exciting the plasma wave requires the laser duration to be at $\tau_{\text{duration}} \approx 1/\omega_p$, where ω_p is the natural plasma frequency which scales with the square-root of the plasma density. For typical laboratory plasmas, τ_{duration} was out of reach for the lasers of the time. To overcome this problem several LWPA schemes were devised; the two major ones being the plasma beatwave accelerator and the self-modulated laser accelerator[3]. Although the mechanics of these schemes differed, the underlying principle was to excite the plasma with a beatwave generated by spatio-temporally overlapping two lasers detuned from each other by $2\pi\omega_p$.

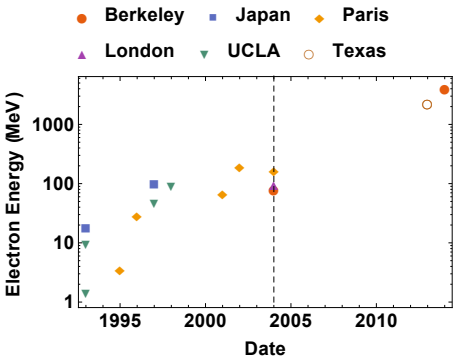

Figure 1: The progress of laser plasma wakefield acceleration by the total energy of the electrons. The dashed line shows the advent of quasi-monoenergetic electrons, until that point the electron bunches had large thermal tails. *This data was gathered from the Web of Science abstract search tool.*

It would require further refinement of laser technology before lasers could directly excite the plasma. Unfortunately, the electron beams generated using these schemes all had broad Maxwellian energy distributions, making them unsuitable for practical applications requiring mono-energetic electrons.

A breakthrough occurred in 2002, when Pukhov predicted the bubble regime in simulation[9]. The bubble regime would solve many of the problems faced by LPWA schemes and is so named as it uses a laser powerful enough to completely expel electrons from the pulse region, creating an ion 'bubble'. One of the most attractive properties of the bubble regime was its predicted ability to produce mono-energetic electrons.

In 2004, this approach bore fruit as three papers, published simultaneously in Nature[10, 11, 12], demonstrated quasi-monoenergetic electron bunches in the bubble regime. In 2006, their results were extended to achieve energies of 1 GeV [13].

In 2013, a group at UT Austin produced a collimated, quasi-monoenergetic electron beam at 2.3 GeV[14], and in 2014, the Esarey group at UC Berkeley produced a 4 GeV[15] beam. These recent developments bring the field within striking distance of the LCLS free electron laser at SLAC, which uses electrons accelerated to 17.4 GeV[2].

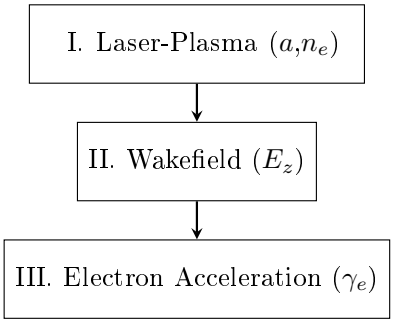

Figure 2: The LWFA process.

[2] Due to the complicated nature of the theory of LPWA in 3D relativistic fields, we will mainly discuss these topics in the linear regime and show the numerical results of their extension into the 3D relativistic regime.

2 The Physics of Laser-Plasma-Acceleration

The LPWA process is divided into three main segments as shown in Figure 2. First the intense laser, characterized by the normalized field strength $a = eA/m_e c^2$, with A as the laser vector potential, interacts with the plasma, characterized by the plasma density n_e. This then produces a longitudinal density modulation, which in turn gives rise to a longitudinal electric wakefield, E_z. The wakefield then accelerates injected electrons to a relativistic energy γ_e. This section reviews these three inter-related phenomena[2].

2.1 The Laser-Plasma Interaction and Creation of Wakefields

The mass of the ions in the plasma is many orders of magnitude larger than the electrons, so it is valid to approximate the plasma as a fluid of mobile electrons against a static background of ions. The motion of the electrons is then governed by the combination of the Lorentz force, the continuity equation, and Poisson's equation. Additionally, if the intensity of the laser is small enough ($a \ll 1$), then these equations can be linearized and are referred to as the cold-fluid equations[16]. In

the cold-fluid regime, the Lorentz force takes the following form:

$$\frac{\partial \mathbf{p}}{\partial t} + (\mathbf{v} \cdot \boldsymbol{\nabla})\mathbf{p} = e\left(\frac{\partial \mathbf{A}}{\partial t} - \mathbf{v} \times \boldsymbol{\nabla} \times \mathbf{A}\right) \tag{1}$$

Where $\mathbf{p}$, $\mathbf{v}$ are the electron's momentum and velocity, and $\mathbf{A}$ is the vector potential of the field.

The linear behaviour of this fluid will be dominated by the force of the electric field on the electrons, accelerating them in the polarization plane. This is called the 'quiver' momentum[3]. Considering the next leading order behaviour of the electron momentum and averaging over one optical cycle, we get a force that is proportional to the intensity gradient of the laser pulse. This is known as the ponderomotive force[3] and can be thought of as the radiation pressure of the laser pulse pushing electrons away from its local space. As the laser propagates through the plasma the ponderomotive force will drive a density wave known as a plasmon, analogous to the physical situation of shooting a cannonball underwater.

[3] So named because the electron will undergo rapid oscillations while its time averaged acceleration will be zero, so it will appear to be quivering

The solution for the density fluctuations in the cold-fluid regime is given by[3]:

$$\left(\frac{\partial^2}{\partial t^2} + \omega_p^2\right)\delta_{n_e} = c^2\nabla^2\frac{a^2}{2} \tag{2}$$

where a is the normalized vector potential, δ_{n_e} is the density fluctuation of the electron fluid and ω_p is the plasma frequency.

Connecting the density fluctuations to the electric field produced using Possion's equation under the assumption of periodic behaviour in $\mathbf{E_z}$ results in the wakefield equation:

$$\mathbf{k} \cdot \mathbf{E_z} = \frac{\delta n_e}{\epsilon_0} \tag{3}$$

Showing that an electric field oriented along the propagation axis will co-propagate π out of phase with the plasmon. We show this in the linear and non-linear 1D regime in Figure 4a. E_z will be the accelerating field that LWPA uses.

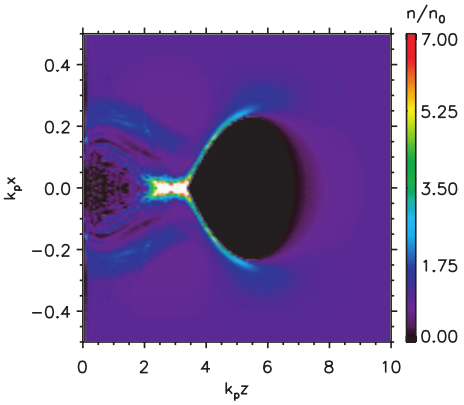

Figure 3: An example of the bubble regime created by a laser pulse with $a = .3$. The laser is moving toward the right, and $\delta_n = \frac{n}{n_0}$, with n being the density of the electrons and n_0 being the density of the ions. The coordinates are dimensionaless and show the evolution of the phase-front.[3]

All modern LWPA approaches operate in the bubble regime so we must extend our linear 1D model to a highly non-linear 2D or 3D model. We can access this regime by relaxing the assumption that $a \ll 1$ and an analytical solution in 1D can still be found[17]. However, in 2D or 3D, the equations become intractable and numerical simulation is required. An example of a numerical solution in a non-linear 2D model is shown in Figure 4b, and an example of the bubble regime is shown in Figure 3.

2.2 Electron Dynamics

Before we can review how electrons are accelerated, we first must discuss how they are trapped in the wakefield.

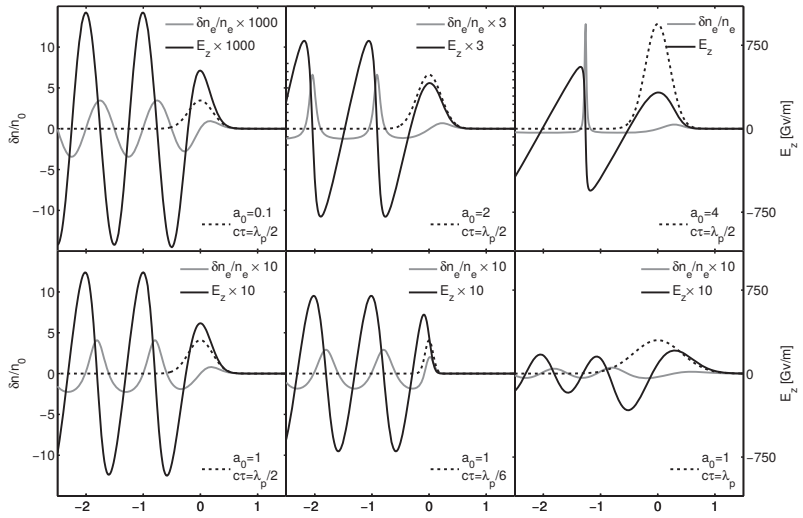

(a) Showing plasmons generated with varying strengths of the peak amplitude of the laser pulse.[18] The laser pulse is the dashed line, the density perturbation is the grey line, and the longitudinal electric field E_z is the black curve. The x-axis is showing the normalized co-ordinate $\xi = kz - wt$, which shows the evolution of the phase-front. Different scenarios are shown: from left to right, the normalized field strength variable ($a = eA/m_e c^2$) is varied, and from top to bottom, the duration of the laser pulse is changed.

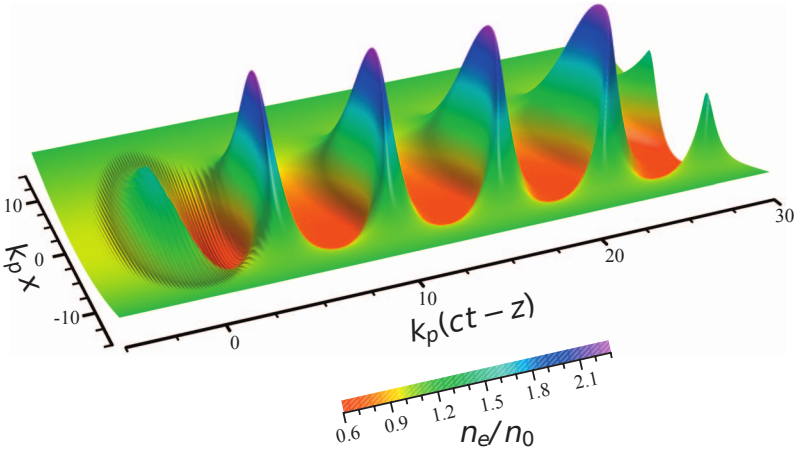

(b) Numerical simulation for a 2D, non-linear model. Many of the features in the 1D model remain– the signature 'leaning' of the density pulse as it becomes non-linear being the most striking.[3]

Figure 4: Plasmons in 1 and 2 dimensions.

2.2.1 Trapping Electrons

In Figure 4a we mentioned that electrons need to be injected into the wakefield. Because the wakefield will be co-propogating with laser pulse –moving close to the speed of light– a stationary electron in the lab frame won't interact with it long enough to be accelerated. To illustrate the point, several phase-space trajectories of test electrons with various initial momenta are shown in Figure 5. Some minimum electron velocity is required and this can either be achieved by externally injecting electrons, or by taking advantage of the non-linear processes in the bubble regime to self-inject electrons from the surrounding fluid[4]. Self-injection is currently favoured by experimentalists as it accelerates the electrons already present in the plasma, allowing the acceleration process to be self-contained.

[4] Interesting, although self-injection happens in non-linear fields in both 1D and 3D, it occurs by different physical processes[19]. We will be focusing on the 3D case in this review.

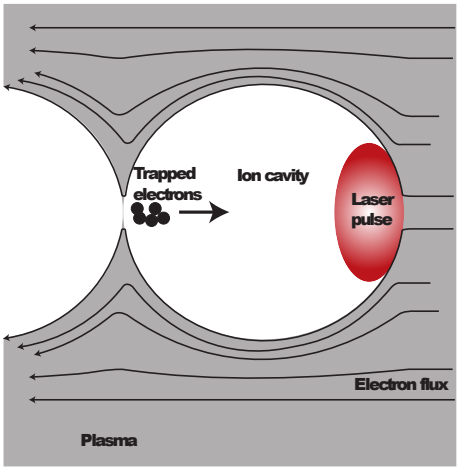

Figure 6: A schematic of the bubble regime.[18]

Although the equations governing the self-injection process in the bubble regime are highly non-linear, a phenomological explanation of the dynamics, considering the bubble as an ion-cavity propogating through an electron fluid, is useful. As the bubble propagates, a small sheath of electrons will form a boundary layer between the ion-cavity and the surrounding electron fluid. A schematic of this is shown in Figure 6

Much like a comet's trajectory can be altered by the Sun's gravitational potential well, the ion-cavity can deflect sheath electrons. An example of this is shown in Figure 7. As it propagates, the bubble's radius will

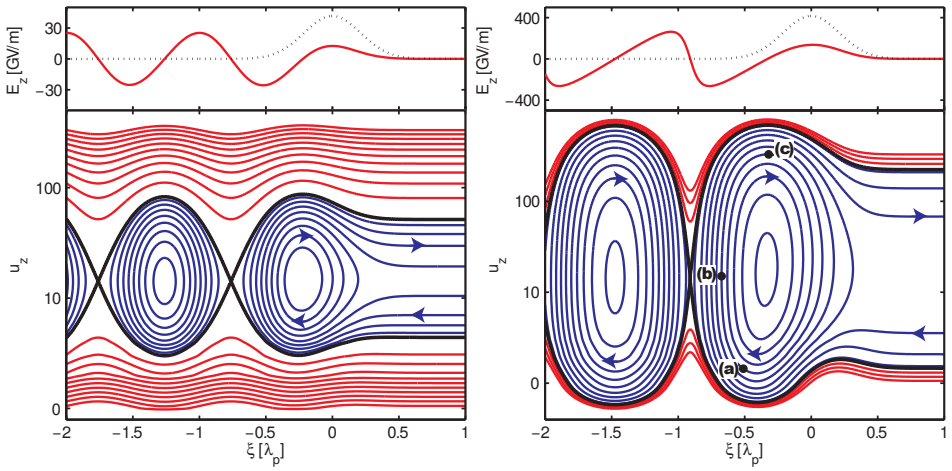

Figure 5: The various trajectories of electrons at different initial normalized momentum ($u_z = p/m_e c^2$) in the reference frame of the laser pulse, which is moving at an relativistic energy $\gamma = 13$ in the lab frame. An electron injected at the phase-space point **a** will be trapped, and accelerated by the wakefield through point **c** until it gains its maximum momentum at point **c**. At point **c**, it will be 'dephased' as it has overtaken the accelerating wakefield, at which point it drops back to point **a**. An experiment has to be designed so that the electrons are harvested at the dephasing point **c**. The black curve is the seprratric, which seperates trapped electrons from untrapped electrons. ξ is the normalized co-ordinate showing the phase-front evolution[18].

change as the front of the laser defocuses and excites a broader swath of the plasma. If the radius changes on timescales much faster than the electron's motion, a trajectory that previously would have been deflected is now within the 'event-horizon' of the bubble and will be trapped. There are strict requirements on the radius of the bubble for this to occur, which additionally imposes constraints on the waist of the laser pulse[20]. An example of the trapping dynamics is shown in Figure 7

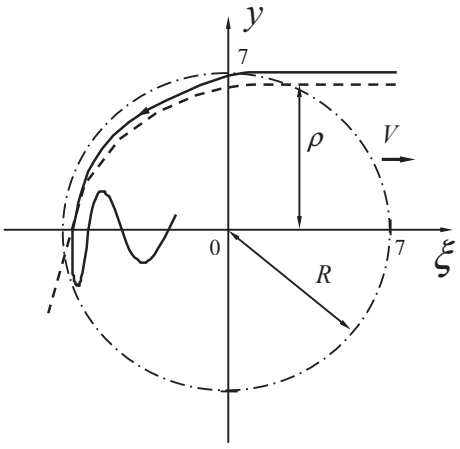

Figure 7: Showing a trapped, and untrapped trajectory of an electron. The bubble parameters are $R = 7$, $\gamma_0 = 4$[21].

Now that we have shown how electrons can be injected into the wakefield, we can discuss the dynamics of their acceleration.

2.3 Electron Acceleration

The plasma bubble sets up a $\mathrm{GeV\,cm^{-1}}$ acceleration field, but the limiting factor in the total energy gain is the distance the electrons are accelerated over. We have already alluded to the dephasing length in Figure 5, where the electron outruns the wakefield. However, there are two additional length scales to be considered.

The first, $L_{\mathrm{PulseDepletion}}$, occurs because the laser-plasma interaction will transfer energy in the initial laser to the plasma wake ultimately dissipating as heat. In 1D, this can be approximated quite well by equating the total energy in the laser to the final energy in the wakefield, getting: $L_{pd} = (E_L/E_z)^2 L$, where E_z is the wakefield and E_L, L refer to the laser field and pulse length, respectively[3].

In the non-linear 3D regime, we consider the pulse depletion as a result of the laser-front being etched away as it excites the wakefield. This etching requires a time scale of ω_p^{-1} to build up, given as $v_{\mathrm{etch}} \approx c\omega_p^2/w_0^2$ [22]. The pump depletion length is then given by:

$$L_{\mathrm{etch}} \approx \frac{c}{v_{\mathrm{etch}}} c\tau_{\mathrm{FWHM}} \approx \frac{c\omega_0^2\tau}{\omega_p^2} \tag{4}$$

The second, $L_{\text{Diffraction}}$ is the most important, as it is the limiting length scale for all modern experiments and is due to inherent laser diffraction. In order to achieve the intense energies necessary for the bubble regime and to meet the requirements on the bubble radius, the lasers need to be focused down to a specific spot size. As soon as this minimum spot size is reached the laser will begin to diffract. The length scale over which this occurs is the Rayleigh length, $L_R = \pi w_0^2/\lambda$, where w_0 is the waist of the laser and λ is the wavelength. The waist will have strict experimental constraints, as it needs to be a certain size for the plasma to enter the bubble regime.

As discussed in Figure 4a, the final length, $L_{\text{Dephasing}}$, is due to the electrons outrunning the wakefield. In 1D, this is defined as the length it takes for the electron's phase to slip by one-half with respect to the plasmon[3]. For the 3D theory theory in the bubble regime, a good approximation of this can be found by estimating the electron's velocity as c, and asking when it will overtake the bubble, which is moving at a slower velocity $v_{\text{group}} - v_{\text{etch}}$. Solving this gives

$$L_d \approx \frac{c}{c - v_\phi} R \approx \frac{2}{3}\frac{\omega_0^2}{\omega_p^2} R. \tag{5}$$

where R is the bubble radius. In Figure 8, we can see the length scales multiplied by the accelerating electric field squared– giving the total energy possible.

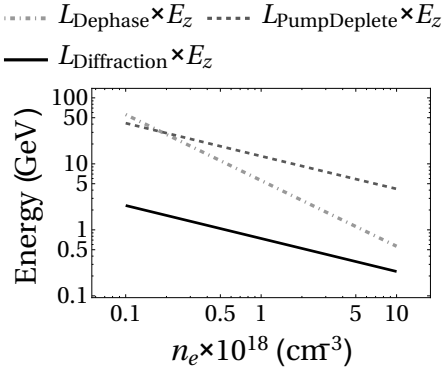

Figure 8: The three length scales involved with accelerating electrons: L_{Dephase} where the electron outruns the wave, self-limiting the total energy gained; $L_{\text{PumpDepletion}}$ where the incident energy in the laser pulse is completely transfered to the wakefield, and the laser can no longer sustain the bubble regime; and $L_{\text{Diffraction}}$ the inherent diffraction of the laser pulse. All lengths are scaled by an accelerating field using parameters from the UT Austin experiment[14], to show the total possible energy an electron could gain.

There are several strategies for extending the length of the laser-plasma interaction. The first and most general is to decrease the plasma density, as seen in Figure 8, the lower the density, the longer the length scales. However, additional strategies are needed to overcome the inherent laser diffraction. To that end we will now discuss the propogation of intense lasers through plasmas, highlighting two main strategies for overcoming laser diffraction.

2.4 Laser Propagation in Plasma

In the previous section we discussed the effect of diffraction as the limiting length scale. However, the plasma itself can dramatically change the propogation of the laser pulse and a clever use of this can overcome diffraction limitations. To first order, we can discuss the plasma's impact on laser propogation through the behaviour of the plasma's index of refraction η given by: $\eta = c^{-1} d\omega/dk$, where ω is the frequency and k is the wavenumber of the laser pulse.

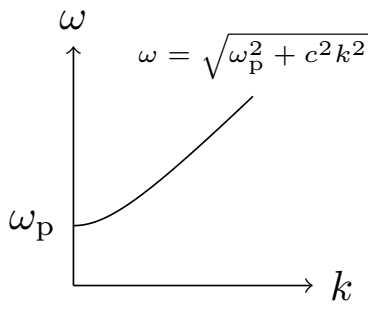

Figure 9: The plasma dispersion relation. We will be dealing with plasmas where $\omega_{\rm p}/\omega << 1$, so to first order the laser will be dispersionless.

$$\eta = \left(1 - \frac{\omega_p (n_e)^2}{\omega^2}\right)^{1/2}. \tag{6}$$

The most important scaling behaviour of η is with the electron's mass

and density. ω_p will scale as $\sqrt{n_e/m_e}$, so η will scale as:

$$\eta = \left(1 - \frac{n_e}{m_e}\frac{e^2}{\epsilon_0 \omega}\right)^{1/2} \tag{7}$$

Recalling that a converging lens has $d\eta/dr < 0$, the plasma will be able to counteract diffraction in two ways: if $dn_e/dr < 0$ or $dm_e/dr > 0$.

As we discussed in Section 2.1, the first order effect of the laser will accelerate them in the polarization plane: the quiver momentum. The electrons will have a maximum amount of kinetic energy passing through the centre of the laser pulse and due to relativity this corresponds to an increase in mass. Thus, the effective mass of the electrons will have $dm_e/dr < 0$ and the plasma will act as a focusing lens. However, in order to use self-focusing to counteract diffraction, the laser has to be intense enough to meaningfully change the electron mass. This condition has been found to be $P[\mathrm{GW}] > 17.5\left(\frac{\omega}{\omega_0}\right)$ [23, 24].

There are several subtleties involved with relativistic self-focusing; chief among these is the effect of pulse length on relativistic self-focusing. The electrons are responding to the laser at frequency ω_p, so it takes time scales on the order of $\tau_p = \frac{1}{2\pi\omega_p}$ for the relativistic effect to build up, ie. the middle of the laser pulse will be 'seeing' the relativistic index gradient created by the front of the pulse. This has two main consequences: first, long pulses, $\tau_{\mathrm{duration}} > \tau_p$, are more susceptible to relativistic effects, and, second, the front of the pulse will be constantly

diffracting away. Groups that primarily use relativistic self-focusing, such as the UT Austin group, not only have to choose laser pulses that are intense enough, but also that are long enough.

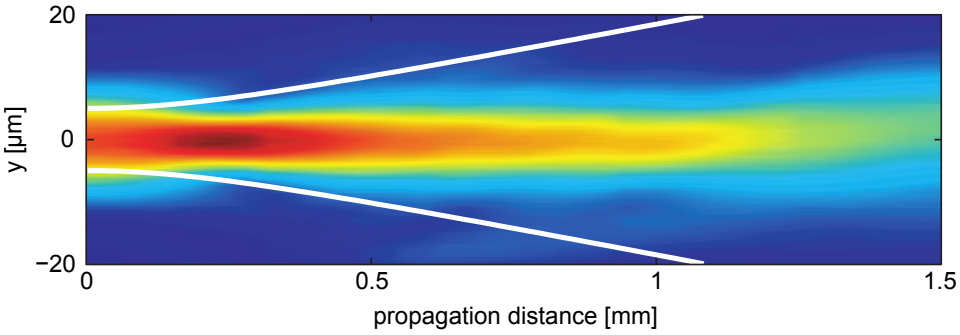

Figure 10: A numerical simulation showing how the relativistic motion of the electrons can cause focusing effects[18]. The white curve shows the diffraction that would have occured in vaccuum. Self-focusing can extend $L_{\text{Diffraction}}$ over many Rayliegh lengths.

However, from Equation (7) we can see that a direct modulation of the electron density can also achieve focusing effects. As long as the density goes as $dn_e/dr > 0$, we have the appropriate condition for a converging lens. This approach is taken by the UC Berkeley group, where a plasma channel is used to give the appropriate density modulation. The plasma channel is a simple tube containing hydrogen gas with a metal plate at each end. A voltage is applied across the length of the tube, ionizing the gas. The gas will cool down more rapidly along the edges of the tube, and this will give rise to an approximately parabolic density profile of the hydrogen gas[25, 26]. It is this parabolic density profile that will act as the focusing lens of the plasma wave.

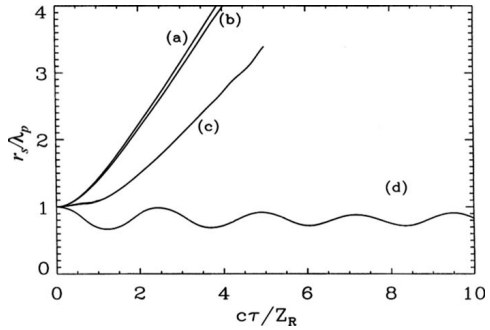

(a) A simulation showing the laser spot size r_s vs normalized propogationg distance $c\tau/L_{\text{Raleigh}}$ for (a) vacuum diffraction, (b) a short pulse in plasma, (c) a long pulse, intense enough to self-focus, and (d) a pulse guided by a plasma channel.[27]

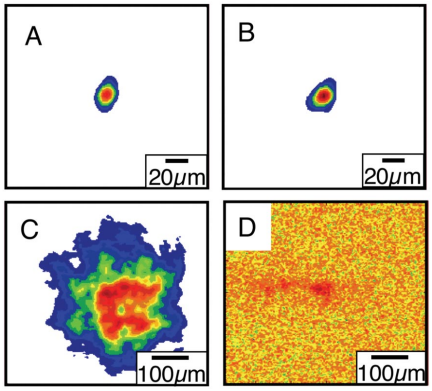

(b) The input mode (a) and output mode (b) of a laser ($I \approx 2P_{\text{critical}}$) are nearly identical after many diffraction lengths. Vacuum propogating over the same distance in (c). Although the laser was firmly within the self-focusing regime, diffraction was actually enhanced over these distances (d)– alluding to the difficulties in controlling self-focusing.[28]

Figure 11: Simulations showcasing the ultility of plasma-channel guiding schemes.

The evolution of a laser pulse in a plasma channel is shown in Figure 11.

3 Experimental Set-Up and State-of-the-Art

Now that we have discussed the underlying physics and given an overview of the experimental constraints faced by modern researchers, we will highlight the recent results of two groups, UT Austin and University of California Berkeley. These two groups are on the forefront of gener-

ating high-energy electrons through LWPA.

3.1 UT Austin

In 2013, the UT Austin group reported a collimated beam of 2 GeV[14]. By leveraging the new petawatt laser facility at UT Austin they were able to arrive firmly within the experimental constraints for relativistic self-guiding. However, due to the intense non-linear interactions involved, detailed numerical work had to be done to find initial conditions that would produce an optimal beam. One such example is shown in Figure 12[14], where by altering initial conditions such as beam profile, startlingly different dynamics occurred.

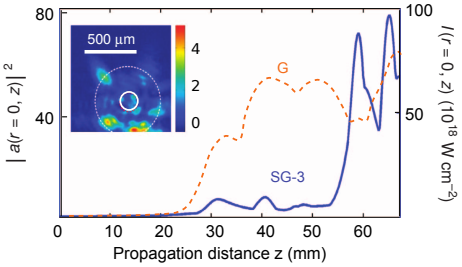

Figure 12: Simulations done by the UT Austin group using the WAKE code showing clear features of self-focusing.[14] As the normalized laser-intensity gets larger, the pulse is contracting–concentrating more of its energy over a smaller area. Interestingly, the self-focusing exhibits a periodic structure– going through two cycles of diffraction-focusing for the super-Gaussian pulse.

Numerical modeling predicted the initial conditions needed by the UT Austin to obtain high-quality mono-energetic beams [29]. Although they were not able to produce the predicted energies, this approach was still successful, as they were able to double the energies of previous results[30]. However, their experiment revealed some discrepancies with the numerical work, as they saw robust self-injection with a non-uniform spot geometry.

Shown in Figure 13 is the experimental setup for UT Austin. At its heart, it is a high-intensity laser hitting an ionized gas. The majority of the experiment is the diagnostics, which allow the team to determine the energy and angular spread of the electrons.

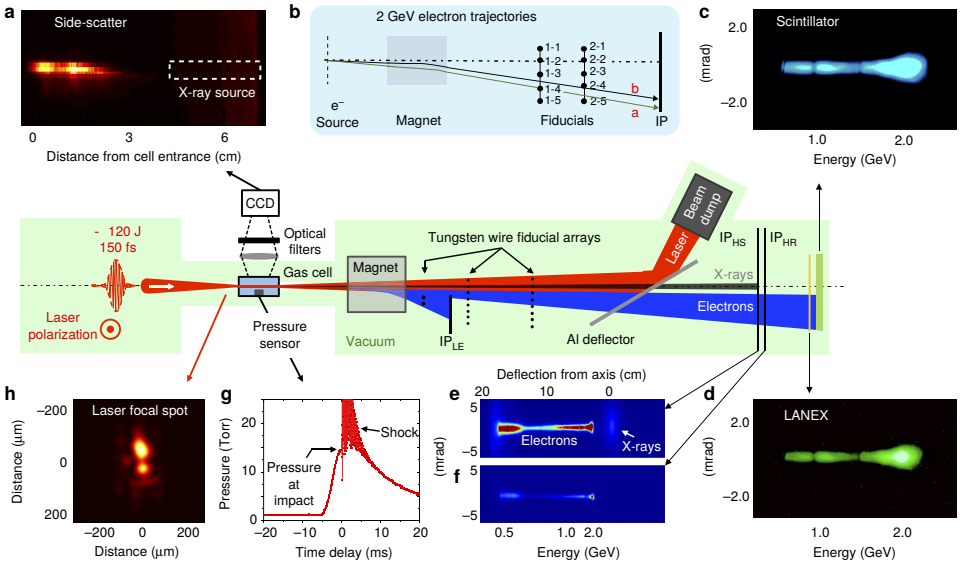

Figure 13: The experimental setup of the UT Austin group.[14] *This figure is reproduced from Nat. Commun. Vol. 4, 2013.* The laser hits a gas cell. It will propagate in the plasma, until the self-focusing process reaches a critical point, where the laser-plasma will enter the bubble regime. (a) Detector to measure sidescatted light from gas-laser interaction. (b) Schematic showing how the electrons are bent using a magnet– acting like a spatial filter for momentum. There are tungsten posts that will cast 'shadows' on the electron detector, allowing the source of the electrons to be backtracked. (c) Electron spectrum on the scintillator. (d) Another spectrum on the LANEX. (e)&(f) X-ray beam blocker. (g) Pressure sensor on the gas cell. (h) Image of the laser spot-size.

The UT Austin group is now developing strategies to increase the energy of the electron beam. Further progress can only be made with an increased understanding of the dynamics of the laser-plasma acceleration, specifically relativistic self-focusing and self-injection, and to that end they have developed novel imaging techniques that, taken together with numerical simulations, form a powerful platform for moving forward.[31, 32]

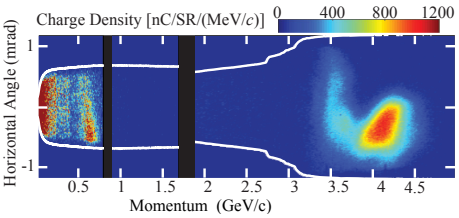

Figure 14: The energy spectrum for the recent Berkeley result.

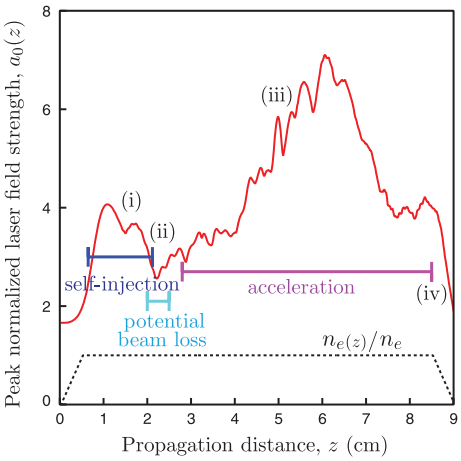

Figure 15: Evolution of the peak normalized intensity of the laser pulse, ($a_0(z)$ done using a particle-in-cell simulation for a top-hat laser pulse with energy 16 J, through a 9 cm plasma waveguide. *From Leemans et. al. 2014 [15]*

3.2 UC Berkeley

In 2014, the Berkeley group reported a collimated electron beam with peak energy of 4.2 GeV. They achieved this through a slightly different experimental philosophy than the UT Austin group. By using lower intensity short-duration lasers, they are able to use a plasma-channel guide that may be damaged by higher-intensity lasers. Although relativistic self-focusing is still required to achieve the high-intensities needed for the bubble regime, the plasma-channel does the majority of the work in preventing laser diffraction. Their use of a lower intensity laser has two main benefits. First, they gain on energy conversion efficiency. As though the acceleration gradients are smaller, they are able to guide them over larger distances. Second, because the laser is lower intensity, the dynamics of self-focusing and non-linear laser-plasma interactions are less pronounced, simplifying the dynamics of the laser propogation. However, they will ultimately be limited by the pump-depletion length, as the laser simply has less energy than the UT Austin petawatt laser.

4 Conclusion

In this review, we have discussed the basic physics processes of LWPA and summarized two approaches for electron acceleration: the high-

intensity, relativistically guiding approach used by UT Austin; and the low-intensity, plasma-channel guided approach used by Berkeley.

For further progress to be made in the field there needs to be a better understanding of the laser-plasma interaction. The new imaging techniques at UT Austin, which allow in vivo imaging of the evolution of the laser and plasmon, is a key contribution as it allows direct comparison to numerical simulations. This is invaluable in efforts to harness the phenomena of self-injection and self-focusing for LWPA technology and an exciting opportunity to develop and refine numerical approaches.

With the current record of 4.2 GeV, LWPA technology is within striking distance of current linear accelerator technology, and with the dynamic progress being made across the entire field, it is clear that LWPA will soon be able to make a broad impact in the scientific community. The raw power exists to accelerate electrons to high GeV energies, all we need to do is control it.

References

[1] JW Wang and GA Loew. Field emission and rf breakdown in high-gradient room-temperature linac structures. *SLAC PUB*, 7684, 1997.

[2] Max Cornacchia. The coherent light source project at slac. In *MULTIPHOTON PROCESSES: ICOMP VIII: 8th International Conference*, volume 525, pages 623–631. AIP Publishing, 2000.

[3] E. Esarey, C. B. Schroeder, and W. P. Leemans. Physics of laser-driven plasma-based electron accelerators. *Rev. Mod. Phys.*, 81:1229–1285, Aug 2009.

[4] Patrick G O'Shea and Henry P Freund. Free-electron lasers: status and applications. *Science*, 292(5523):1853–1858, 2001.

[5] Claudio Pellegrini and Joachim Stöhr. X-ray free-electron laser-sprinciples, properties and applications. *Nuclear Instruments and Methods in Physics Research Section A: Accelerators, Spectrometers, Detectors and Associated Equipment*, 500(1):33–40, 2003.

[6] Brian WJ McNeil and Neil R Thompson. X-ray free-electron lasers. *Nature photonics*, 4(12):814–821, 2010.

[7] T. Tajima and J. M. Dawson. Laser electron accelerator. *Phys. Rev. Lett.*, 43:267–270, Jul 1979.

[8] Sterling Backus, Charles G Durfee III, Margaret M Murnane, and Henry C Kapteyn. High power ultrafast lasers. *Review of scientific instruments*, 69(3):1207–1223, 1998.

[9] Alexancer Pukhov and Jürgen Meyer-ter Vehn. Laser wake field acceleration: the highly non-linear broken-wave regime. *Applied*

Physics B, 74(4-5):355–361, 2002.

[10] SPD Mangles, CD Murphy, Z Najmudin, AGR Thomas, JL Collier, AE Dangor, EJ Divall, PS Foster, JG Gallacher, CJ Hooker, et al. Monoenergetic beams of relativistic electrons from intense laser–plasma interactions. *Nature*, 431(7008):535–538, 2004.

[11] Jérôme Faure, Yannick Glinec, A Pukhov, S Kiselev, S Gordienko, E Lefebvre, J-P Rousseau, F Burgy, and Victor Malka. A laser–plasma accelerator producing monoenergetic electron beams. *Nature*, 431(7008):541–544, 2004.

[12] C. G. R. Geddes, Cs Toth, J. van Tilborg, E. Esarey, C. B. Schroeder, D. Bruhwiler, C. Nieter, J. Cary, and W. P. Leemans. High-quality electron beams from a laser wakefield accelerator using plasma-channel guiding. *Nature*, 431(7008):538–541, Sep 2004.

[13] W. P. Leemans, B. Nagler, A. J. Gonsalves, Cs Toth, K. Nakamura, C. G. R. Geddes, E. Esarey, C. B. Schroeder, and S. M. Hooker. Gev electron beams from a centimetre-scale accelerator. *Nat Phys*, 2(10):696–699, Oct 2006.

[14] Xiaoming Wang, Rafal Zgadzaj, Neil Fazel, Zhengyan Li, S. A. Yi, Xi Zhang, Watson Henderson, Y.-Y. Chang, R. Korzekwa, H.-E. Tsai, C.-H. Pai, H. Quevedo, G. Dyer, E. Gaul, M. Martinez, A. C. Bernstein, T. Borger, M. Spinks, M. Donovan, V. Khudik, G. Shvets, T. Ditmire, and M. C. Downer. Quasi-monoenergetic

laser-plasma acceleration of electrons to 2 gev. *Nat Commun*, 4, Jun 2013. Article.

[15] P. Leemans, W. J. Gonsalves, A. H.-S. Mao, K. Nakamura, C. Benedetti, B. Schroeder, C. Cs. Tóth, J. Daniels, E. Mittelberger, D. S. Bulanov, S. J.-L. Vay, C. G. R. Geddes, and E. Esarey. Multi-gev electron beams from capillary-discharge-guided subpetawatt laser pulses in the self-trapping regime. *Phys. Rev. Lett.*, 113:245002, Dec 2014.

[16] LM Gorbunov and VI Kirsanov. Excitation of plasma waves by an electromagnetic wave packet. *Sov. Phys. JETP*, 66(290-294):40, 1987.

[17] P Sprangle, E Esarey, and A Ting. Nonlinear theory of intense laser-plasma interactions. *Physical review letters*, 64(17):2011, 1990.

[18] Guillaume Genoud. *Laser-Driven Plasma Waves for Particle Acceleration and X-Ray Production.* PhD thesis, Lund University, 2011.

[19] Eric Esarey and Mark Pilloff. Trapping and acceleration in nonlinear plasma waves. *Physics of Plasmas (1994-present)*, 2(5):1432–1436, 1995.

[20] I. Kostyukov, E. Nerush, A. Pukhov, and V. Seredov. Electron

self-injection in multidimensional relativistic-plasma wake fields. *Phys. Rev. Lett.*, 103:175003, Oct 2009.

[21] I Kostyukov, E Nerush, A Pukhov, and V Seredov. Electron self-injection in multidimensional relativistic-plasma wake fields. *Physical review letters*, 103(17):175003, 2009.

[22] C. D. Decker, W. B. Mori, K.C. Tzeng, and T. Katsouleas. The evolution of ultraintense, shortpulse lasers in underdense plasmas. *Physics of Plasmas (1994-present)*, 3(5):2047–2056, 1996.

[23] P Sprangle, Cha-Mei Tang, and E Esarey. Relativistic self-focusing of short-pulse radiation beams in plasmas. *Plasma Science, IEEE Transactions on*, 15(2):145–153, 1987.

[24] Guo-Zheng Sun, Edward Ott, YC Lee, and Parvez Guzdar. Self-focusing of short intense pulses in plasmas. *Physics of Fluids (1958-1988)*, 30(2):526–532, 1987.

[25] A. Butler, D. J. Spence, and S. M. Hooker. Guiding of high-intensity laser pulses with a hydrogen-filled capillary discharge waveguide. *Phys. Rev. Lett.*, 89:185003, Oct 2002.

[26] D. J. Spence and S. M. Hooker. Investigation of a hydrogen plasma waveguide. *Phys. Rev. E*, 63:015401, Dec 2000.

[27] P Sprangle, E Esarey, J Krall, and G Joyce. Propagation and guiding of intense laser pulses in plasmas. *Physical review letters*,

69(15):2200, 1992.

[28] CGR Geddes, Cs Toth, J Van Tilborg, E Esarey, CB Schroeder, J Cary, and WP Leemans. Guiding of relativistic laser pulses by preformed plasma channels. *Physical review letters*, 95(14):145002, 2005.

[29] Serguei Y Kalmykov, Sunghwan A Yi, Arnaud Beck, Agustin F Lifschitz, Xavier Davoine, Erik Lefebvre, Alexander Pukhov, V Khudik, Gennady Shvets, Steven A Reed, et al. Numerical modelling of a 10-cm-long multi-gev laser wakefield accelerator driven by a self-guided petawatt pulse. *New Journal of Physics*, 12(4):045019, 2010.

[30] M. Tzoufras, S. Tsung, F. B. Mori, W. and A. Sahai, A.˙ Improving the self-guiding of an ultraintense laser by tailoring its longitudinal profile. *Phys. Rev. Lett.*, 113:245001, Dec 2014.

[31] Peng Dong. Laboratory visualization of laser-driven plasma accelerators in the bubble regime, 2010.

[32] Zhengyan Li, Rafal Zgadzaj, Xiaoming Wang, Yen-Yu Chang, and Michael C Downer. Single-shot tomographic movies of evolving light-velocity objects. *Nature communications*, 5, 2014.